Data-driven ion-independent relative biological effectiveness modeling using the beam quality Q

IOP Publishing Phys. Med. Biol. 68 (2023) 105009 https://doi.org/10.1088/1361-6560/acc9f9

Physics in Medicine & Biology

IPEM Institute of Physics and Engineering in Medicine

RECEIVED
31 October 2022

REVISED
24 March 2023

ACCEPTED FOR PUBLICATION
3 April 2023

PUBLISHED
8 May 2023

PAPER

Data-driven ion-independent relative biological effectiveness modeling using the beam quality Q

Liheng Tian and **Armin Lühr**

TU Dortmund University, Department of Physics, Dortmund, Germany

E-mail: Liheng.Tian@tu-dortmund.de

Keywords: ion therapy, RBE modeling, beam quality, LET, proton therapy

Supplementary material for this article is available online

Abstract

Beam quality $Q = Z^2/E$ (Z = ion charge, E = energy), an alternative to the conventionally used linear energy transfer (LET), enables ion-independent modeling of the relative biological effectiveness (RBE) of ions. Therefore, the Q concept, i.e. different ions with similar Q have similar RBE values, could help to transfer clinical RBE knowledge from better-studied ion types (e.g. carbon) to other ions. However, the validity of the Q concept has so far only been demonstrated for low LET values. In this work, the Q concept was explored in a broad LET range, including the so-called overkilling region. The particle irradiation data ensemble (PIDE) was used as experimental *in vitro* dataset. Data-driven models, i.e. neural network (NN) models with low complexity, were built to predict RBE values for H, He, C and Ne ions at different *in vitro* endpoints taking different combinations of clinically available candidate inputs: LET, Q and linear-quadratic photon parameter α_x/β_x. Models were compared in terms of prediction power and ion dependence. The optimal model was compared to published model data using the local effect model (LEM IV). The NN models performed best for the prediction of RBE at reference photon doses between 2 and 4 Gy or RBE near 10% cell survival, using only α_x/β_x and Q instead of LET as input. The Q model was not significantly ion dependent ($p > 0.5$) and its prediction power was comparable to that of LEM IV. In conclusion, the validity of the Q concept was demonstrated in a clinically relevant LET range including overkilling. A data-driven Q model was proposed and observed to have an RBE prediction power comparable to a mechanistic model regardless of particle type. The Q concept provides the possibility of reducing RBE uncertainty in treatment planning for protons and ions in the future by transferring clinical RBE knowledge between ions.

1. Introduction

Compared to conventional photon therapy, ion therapy is characterized by, first, an energy deposition peak at the end of its range, called the Bragg peak, and, second, an increased relative biological effectiveness (RBE). While the RBE of certain ions, e.g. carbon, has been studied in some detail for decades (Raju and Carpenter 1978, Hawkins 1996, Ando and Kase 2009, Mizoe *et al* 2012), more research on other particles is desired. For example, a constant RBE of 1.1 is widely applied for proton beam therapy (Heuchel *et al* 2022, Paganetti *et al* 2019) but variable clinical proton RBE has been reported (Connor *et al* 2017, Lambrecht *et al* 2018, Bahn *et al* 2020, Underwood *et al* 2022, Eulitz *et al* 2019, 2023). In addition to particles that have already been applied clinically, i.e. proton and carbon, new applications using e.g. helium (Mein *et al* 2019), oxygen (Chang *et al* 2014) and multi-ion beams (Ebner *et al* 2021) are emerging. An ion-independent model, would help to enrich the data pool by assembling data of different ions and to transfer knowledge from better-investigated ones. In order to quantify and predict RBE, different RBE models have been proposed. Phenomenological proton RBE models (Tilly *et al* 2005, Carabe-Fernandez *et al* 2007, Wedenberg *et al* 2013, McNamara *et al* 2015, Mairani *et al* 2017, McMahon 2021) were built by fitting fixed formulas on the RBE data for protons. For these models, the transferability of their specific formalism needs to be verified against clinical data as the clinical endpoint differs from the biological *in vitro* endpoint used for modeling. Furthermore, these models are driven by linear energy transfer (LET), which only quantifies the integral energy deposition while ignoring the microdosimetric features of the beam; thus, it can hardly be used for the many different ions that are naturally involved in clinical ion beams. Mechanistic models, e.g. the local effect model (LEM) (Scholz *et al* 1997, Friedrich *et al* 2012) and the microdosimetric–kinetic Model (Hawkins 1998), take into account the microdosimetric features and are based on generally believed mechanisms, including that the enhanced RBE of ions is determined by the microscopic dose distribution in the cell nucleus. However, some quantities required for those models, e.g. the cell nucleus size or microscopic dose distribution (nanometer scale) (Kase *et al* 2008), may be difficult to determine in clinical application.

Recently, a new concept, namely, beam quality Q was proposed for RBE modeling (Lühr *et al* 2017, Tian *et al* 2022). The beam quality is defined as $Q = Z^2/E$, with Z and E being the ion's charge and kinetic energy per nucleon, respectively. It has been shown that a Q-driven model is able to predict the RBE, regardless of ion type and for individual ions, comparable to another widely used ion-specific model (Tian *et al* 2022). This opens up the possibility of using RBE data from different ions for model building and thereby improving the precision of RBE predictions. However, the proposed Q-dependent model is a simple linear model and, thus, only works in the region of low to intermediate Q values, i.e. for LET values below the so-called overkilling region (Tian *et al* 2022). Accordingly, the general validity of the ion-independent Q concept still needs to be shown.

Therefore, the purpose of this work was, first, to demonstrate the validity of the ion-independent Q concept for a broad LET range including larger Q values and the overkill domain and, second, to propose an experimental data-driven, non-linear Q model describing the RBE for different ions while focusing on clinically available input variables.

2. Material and methods

2.1. PIDE dataset and data selection

The particle irradiation data ensemble (PIDE, version 3.2) (Friedrich *et al* 2021), consisting of a dataset recording the *in vitro* experimental data of cell survival experiments of 115 publications covering 1118 data points of 21 types of ion irradiation, was used in this work.

The following data selection criteria were applied. Data from experiments with monoenergetic irradiation of ions no heavier than neon ($Z < 11$) were considered. The minimum kinetic energy thresholds for different ions were chosen such that the ion ranges in water were at least 25 μm (Lühr *et al* 2012), i.e. in the order of the size of a single cell. In addition, only experiments with positive and finite α_x/β_x and an asynchronous cell cycle were considered. Here, α_x and β_x are the α and β parameters of the linear-quadratic (LQ) model of photon irradiation. Irradiation data of a specific ion were only considered if at least five data points were available for that ion. One proton data point with an α_x/β_x value much higher (~70 Gy) than those of all others (<30 Gy) was excluded in this work. Consequently, irradiation data of the following ions were selected: proton (48 data points), helium (30), carbon (148) and neon (58) with a minimum energy of 1.03, 2.29, 4.07 and 5.04 A·MeV, respectively. In the following, this selected dataset is called the PIDE dataset for simplicity.

For each PIDE record, an LET value was provided. These LET values were directly taken for this study, i.e. regardless of their definition as, e.g. dose or track averaged LET. The Q values were calculated using the energy E and charge Z values recorded in the PIDE. Some of the experimental publications covered by the PIDE only provide either an E or LET value. The missing values were calculated by the PIDE group based on the reported counterpart values using the software ATIMA (Geissel *et al* 2002, Friedrich *et al* 2021). Two types of α and β values are recorded in the PIDE: first, the data originally reported by the experimenters and, second, the data retrospectively obtained by the PIDE group using the LQ model fitting of the underlying radiation response data. In this work, only the originally reported data were used.

RBE values at an isoeffective photon dose d_x, RBE_{dx}, were calculated for d_x ranging from 1 to 30 Gy using the LQ model formalism (cf appendix) and α_x, β_x, α_i and β_i values as recorded in the PIDE. The maximum and minimum RBE values given by $RBE_{max} = \alpha_i/\alpha_x$, $RBE_{min} = \sqrt{\beta_i/\beta_x}$ (Carabe-Fernandez *et al* 2007, Dale *et al* 2009) were also considered and could be regarded approximately as RBE_0 and RBE_∞ at d_x approaching 0 and ∞, respectively. Thus, the RBE_{dx} values derived from the experimental α_x, β_x, α_i and β_i values as recorded in the PIDE were regarded as the experimentally derived RBE_{dx} ground truth in this work. RBE values defined by the cell survival S, RBE_S, were also calculated (cf appendix) and modeled for $S = 0.1\%$, 1.0%, 10.0%, 50.0% and 90.0% for discussion.

2.2. Correlation analysis

This work aimed at building a model that takes clinically available variables, i.e. LET, Q and α_x/β_x or combinations thereof, as input and predicts the resulting RBE values. Spearman's correlation coefficient values, ρ, between different potential input variables and output data were calculated using the Python package Pandas (Reback *et al* 2022).

2.3. RBE modeling

A neural network (NN) model was used to perform data-driven RBE modeling to avoid any presumption on the functional form of the RBE model. Considering the limited amount of available data (284 experimental records), a model with a comparably simple architecture was applied, i.e. a fully connected NN consisting of two hidden layers of the size of 6. As activation function, the ReLU (rectified linear unit) was used. The machine learning package scikit-learn (Pedregosa *et al* 2011) was used for the machine-learning application in this work.

Three RBE models with different input variables, i.e. combinations of the physical and biological quantities Q, LET and α_x/β_x, were compared; namely, $RBE_{2Gy}(Q, \alpha_x/\beta_x)$, $RBE_{2Gy}(LET, \alpha_x/\beta_x)$ and $RBE_{2Gy}(Q, LET, \alpha_x/\beta_x)$, respectively, with RBE_{2Gy} was explicitly chosen as an example in this manuscript.

2.4. Model evaluation

The models of $RBE_{2Gy}(Q, \alpha_x/\beta_x)$, $RBE_{2Gy}(LET, \alpha_x/\beta_x)$ and $RBE_{2Gy}(Q, LET, \alpha_x/\beta_x)$ were trained and tested using the same training and test set, respectively. The test set (20% of the total selected dataset) was randomly chosen in the domain of $Q \in (0, 15)$ $(A\cdot MeV)^{-1}$ and $\alpha_x/\beta_x \in (0, 30)$ Gy. The remaining data of the PIDE dataset fulfilling the selection criteria specified in section 2.1 were used as training set. The prediction power of the trained models was compared by means of the coefficient of determination (called r2 score in the following) and the mean square error (MSE) between the predicted and experimentally derived RBE_{2Gy} of the test set regardless of particle type. The ion dependence (95% confidence level) of the models was tested by applying an ANOVA (analysis of variance) test on the residuals between the model calculated and the experimentally derived RBE_{2Gy} of different particles. For the ANOVA test, all eligible PIDE data, i.e. training and test set, were used due to the limited amount of data of individual particles in the test set.

2.5. Uncertainties of the model prediction

The uncertainty of the model prediction in the two-dimensional (2D) space spanned by the two parameters Q and α_x/β_x was evaluated by the following procedure:

(1) randomly divide the PIDE dataset into a training set (80%) and a test set (20%);

(2) train a model using the training set and save model parameters;

(3) repeat (1) and (2) until 100 models based on different training sets are built and saved;

(4) determine the uncertainty of the model by calculating the standard deviation (SD) of the 100 RBE_{2Gy} values calculated by those 100 models at each (grid) point in the 2D space of Q-α_x/β_x.

2.6. Comparison to other RBE models

The prediction of the proposed data-driven model was compared to RBE results of LEM IV for the biological endpoint of 10% survival fraction, i.e., RBE_{10} (Elsässer *et al* 2010) considering radiation data of human salivary gland (HSG) cells reported by (Furusawa *et al* 2000). For the fairness of the comparison, the NN model was re-trained for RBE_{10} and the inputs of Q and α_x/β_x. The data of the HSG cells reported by (Furusawa *et al* 2000, Elsässer *et al* 2010) were used as test set while the remaining PIDE dataset was used for training. The experimentally derived RBE_{10} values were calculated as before by applying the LQ model on PIDE-recorded α_x, β_x, α_i and β_i values (cf appendix). Note that the ion dependence of the model should not be inferred by this analysis as the training and test set were not split randomly.

The prediction of LEM IV was interpolated using the data reported by (Elsässer *et al* 2010).

For the same test data, the prediction of the recently proposed Q-driven linear RBE model (Tian *et al* 2022) was also considered and compared in terms of RBE_{10}. This model is called linear model in the following, as it assumes RBE_{max} to be linear in $Q/(\alpha_x/\beta_x)$. The prediction of RBE_{10} by the linear model is described in the appendix.

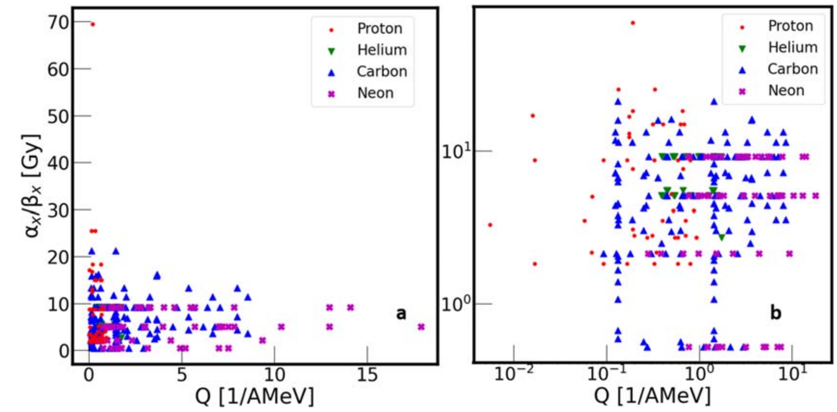

Figure 1. Distribution of the Q and α_x/β_x values of the dataset used in this work using both linear (a) and log–log (b) scale. The ion type is referenced by color and symbol.

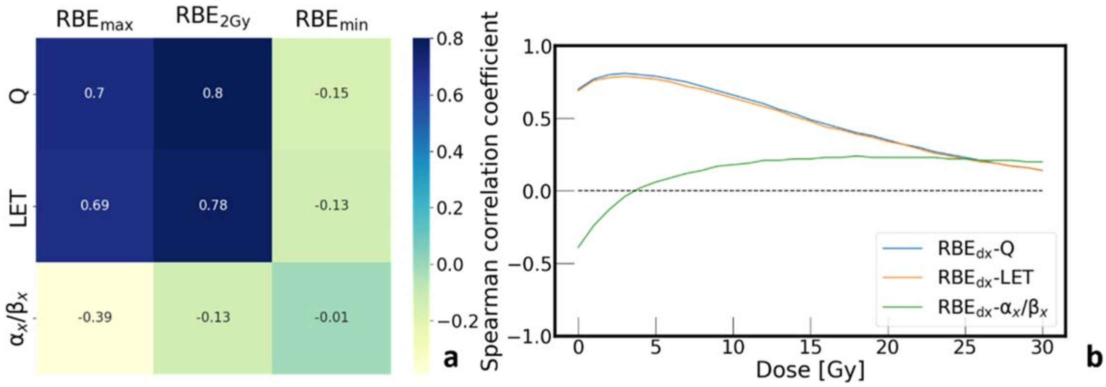

Figure 2. Spearman's correlation values ρ between the candidate input (LET, Q and α_x/β_x) and output (RBE_{dx}) data: (a) correlation map for the three reference photon dose levels d_x of 0 (RBE_{max}), 2 Gy (RBE_{2Gy}) and ∞ (RBE_{min}). (b) ρ between the input variables (LET, Q and α_x/β_x) and RBE_{dx} at dose levels d_x within (0, 30) Gy.

3. Results

3.1. Data distribution

The distribution of data points of the PIDE dataset in the 2D space of Q-α_x/β_x is shown in figure 1. All data, except for one data point for protons (Baggio *et al* 2002) and one for neon ions (Furusawa *et al* 2000), were within the Q interval of (0, 15) $(A\cdot MeV)^{-1}$ and α_x/β_x interval of (0, 26) Gy with a lower data density at high-Q values, especially, when α_x/β_x values were also high.

3.2. Variable correlation

Spearman's correlation coefficients ρ between output (RBE_{dx} at different dose level d_x) and clinically available input variables (LET, Q and α_x/β_x) are presented in figure 2. The ρ between RBE_{dx} and either Q or LET were comparable, while the ρ between RBE_{dx} and α_x/β_x was low. The ρ between RBE_{dx} and LET or Q were highest for d_x values within the photon reference dose interval 2–4 Gy. Hence, RBE_{dx} within 2–4 Gy was regarded as the most 'predictable' output.

In line with this finding, the prediction of the RBE_{dx} for d_x values between 2 and 4 Gy was observed to be better than that for d_x in other domains, i.e. (0, 2) Gy and (4, ∞) Gy. As this is a dose range of particular clinical relevance, results presented in this work focus on the prediction of RBE within this dose domain (cf comparison between the prediction of RBE for different d_x domains in the appendix).

3.3. Comparison of models using different input

The ability of the RBE_{2Gy}(Q, α_x/β_x) model to predict the experimentally derived RBE_{2Gy} values is shown in figure 3. The same comparison for the two other models, namely RBE_{2Gy}(LET, α_x/β_x) and RBE_{2Gy}(Q, LET,

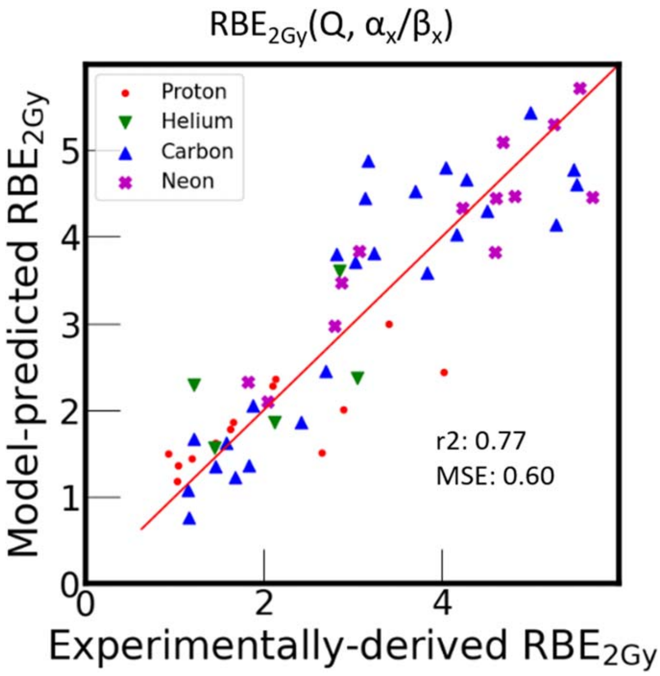

Figure 3. Comparison between the predicted $RBE_{2Gy}(Q, \alpha_x/\beta_x)$ and experimentally derived RBE_{2Gy} values for the test dataset. The ion type is color coded. The reference red line demonstrates $y = x$, i.e. the ideal case that the prediction equals the corresponding experiment.

Table 1. Performance of the neural network models using different inputs to predict RBE_{2Gy}: coefficient of determination (r2 score), mean square error (MSE), p value of ANOVA test and the results of corresponding ion-dependence test.

Models	r2 score	MSE	p (ANOVA)	Ion dependence
$RBE_{2Gy}(LET, Q, \alpha_x/\beta_x)$	0.77	0.60	0.13	Not significant
$RBE_{2Gy}(Q, \alpha_x/\beta_x)$	0.77	0.60	0.58	Not significant
$RBE_{2Gy}(LET, \alpha_x/\beta_x)$	0.74	0.68	2.1×10^{-5}	Significant

α_x/β_x), is shown in supplementary figure S1. A comparison between the model calculated RBE_{2Gy} by both $RBE_{2Gy}(Q, \alpha_x/\beta_x)$ and $RBE_{2Gy}(LET, \alpha_x/\beta_x)$ for the entire dataset are shown in figure S3.

The model performance of the $RBE_{2Gy}(LET, \alpha_x/\beta_x)$, $RBE_{2Gy}(Q, \alpha_x/\beta_x)$ and $RBE_{2Gy}(Q, LET, \alpha_x/\beta_x)$ models is compared in table 1 regarding the r2 score, the MSE between the experimentally derived and modeled RBE_{2Gy} and the result of the ANOVA test. Note that, according to the result of the ANOVA test, the model of $RBE_{2Gy}(LET, \alpha_x/\beta_x)$ cannot provide ion-independent predictions, i.e. the model cannot make predictions equally for different ions, even for the training set. Thus, measurement of the prediction power, i.e. r2 score and MSE, should be regarded as invalid, although corresponding numbers could still be obtained and compared to the other two models.

Considering the models of $RBE_{2Gy}(Q, LET, \alpha_x/\beta_x)$ and $RBE_{2Gy}(Q, \alpha_x/\beta_x)$, their r2 scores and MSE were comparable and both models were not significantly dependent on ion type. The differences (mean ±SD) between the predictions of the two models $RBE_{2Gy}(Q, \alpha_x/\beta_x)$ and $RBE_{2Gy}(Q, LET, \alpha_x/\beta_x)$ for the same data point (0.00 ± 0.11) were much smaller than the differences between the model $RBE_{2Gy}(Q, \alpha_x/\beta_x)$ and the respective experimental data points (-0.03 ± 0.67), as shown in supplementary figure S2. That means adding LET as an additional variable did not substantially change or improve the predicted RBE_{2G} values. Therefore, adding LET to the model cannot substantially decrease the observed differences between individual experimental data points and predictions.

The performance of $RBE_S(Q, \alpha_x/\beta_x)$ defined by cell survival is shown in table A2 in the appendix and is consistent with the performance of $RBE_{dx}(Q, \alpha_x/\beta_x)$. The r2 score was shown to be highest in the domain near 10% survival fraction; while at all survival fraction levels, the models were not significantly ion dependent.

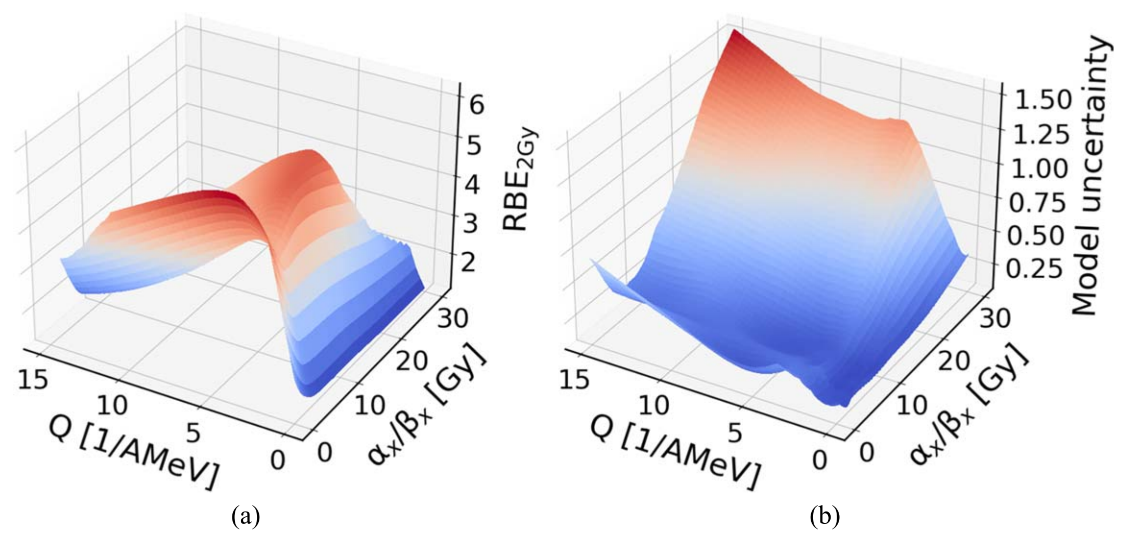

Figure 4. $RBE_{2Gy}(Q, \alpha_x/\beta_x)$ model in the Q and α_x/β_x space: (a) mean and (b) standard deviation of 100 trained $RBE_{2Gy}(Q, \alpha_x/\beta_x)$ models. Note that model predictions with uncertainties larger than 0.5 are not displayed.

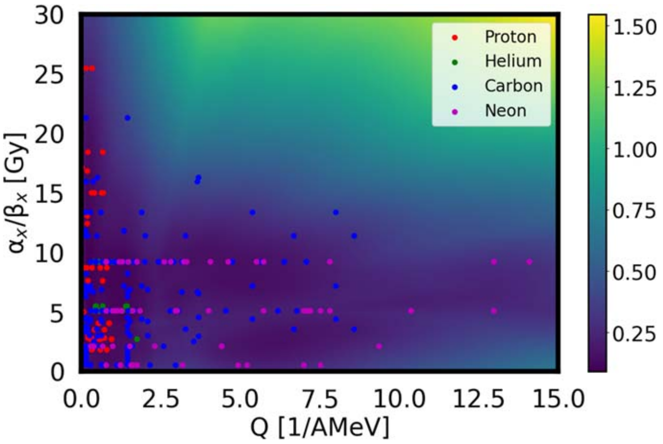

Figure 5. Color map of the RBE_{2Gy} standard deviation of 100 trained $RBE_{2Gy}(Q, \alpha_x/\beta_x)$ models with an overlay of the experimental data points, which are color coded by ion type. The standard deviation is particularly high in regions with no experimental data points.

3.4. Model uncertainties

Figure 4 shows the mean and SD values resulting from the 100 trained $RBE_{2Gy}(Q, \alpha_x/\beta_x)$ models in the 2D space of Q and α_x/β_x. RBE_{2Gy} was observed to increase with increasing Q in the low-Q domain (Q < approx. 3 [A MeV^{-1}]) and to decrease with increasing Q in high-Q domain. This resembles the well-known overkilling effect.

The same SD values are shown in figure 5 as a 2D color map overlaid by the experimental data points from the PIDE dataset. The model uncertainty was observed to be comparably low in regions of high data point density and particularly high in regions where experimental data points were missing.

3.5. Comparison with other RBE models

The experimental RBE_{10} values for HSG cells ($\alpha_x/\beta_x = 5.09$ Gy) irradiated with helium and carbon ions as reported by (Furusawa *et al* 2000) were compared to the model predictions given by LEM IV (Elsässer *et al* 2010) and the present NN model using Q and α_x/β_x. They are shown as a function of LET in figure 6(a). In figure 6(b), the same experimental data and model predictions given by the NN Q model were compared to the earlier proposed linear Q model (Tian *et al* 2022) but shown as a function of $Q/(\alpha_x/\beta_x)$.

For the RBE_{10} of helium and carbon irradiation, the r2 and MSE between the NN model prediction and experimental RBE data were 0.85 and 0.08, respectively (figure 7). For the LEM IV model interpolation, the r2 and MSE were 0.82 and 0.10, respectively. Accordingly, both models were comparable in terms of r2 and MSE. Systematic bias for different particles was observed for both RBE models: for the LEM IV model interpolation,

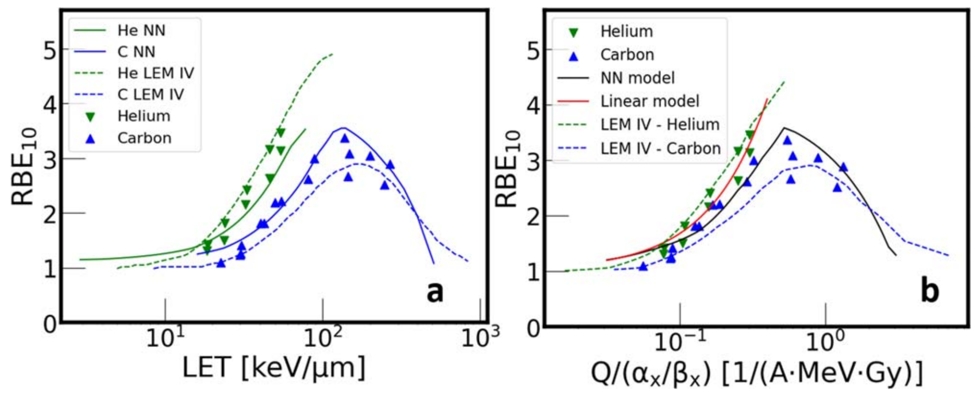

Figure 6. Comparison between the experimentally derived RBE_{10} for the HSG cell line and the model predictions by the neural network (NN) model and the local effect model IV (LEM IV) for different ions as function of (a) LET and (b) $Q/\alpha_x/\beta_x$. For comparison, the linear Q model is also shown in (b). Note that the splitting of data in training and test sets used here was not done following unbiased modeling rule, instead it was done non-randomly for the purpose of fair comparison with LEM IV. Thus, the systematic error seen here is not suitable for the evaluation of ion dependence of the model.

the residuals of helium and carbon RBE_{10} were -0.24 ± 0.17 and 0.22 ± 0.17, respectively. For the NN model prediction, the residual values of helium and carbon RBE_{10} were 0.19 ± 0.28 and -0.15 ± 0.22, respectively.

Both, the NN and the linear Q model were observed to follow a similar trend in the $Q/(\alpha_x/\beta_x)$ interval of (0, 0.4) $(\mathrm{A \cdot MeV \cdot Gy})^{-1}$. However, the linear model cannot predict experimentally derived RBE_{10} data in the domain of overkilling, i.e. for $Q/(\alpha_x/\beta_x)$ larger than 0.4 $(\mathrm{A \cdot MeV \cdot Gy})^{-1}$ in this case.

4. Discussion

In this work, we aimed to test the concept of Q-driven RBE modeling, i.e. irradiation with different ions has similar RBE at similar Q level over a wide LET range, including the domain of so-called overkilling. For this purpose, a data-driven NN model irradiations was built that only takes Q and α_x/β_x as input to predict RBE (defined by either reference photon dose or cell survival level) for different ions. The prediction power was evaluated (coefficient of determination) to be near 0.8 for the RBE defined by either the clinically relevant dose interval of 2–4 Gy or cell survival level of about 10%. No significant ion dependence was found in the Q-based prediction of RBE in the mentioned intervals, i.e. the Q concept was not rejected. In addition, the RBE_{10} prediction was observed to be comparable to LEM IV regarding accuracy and precision. The relevance of a Q model that does not depend on ion type could be the consolidation of clinical RBE research for different ions in the future.

The considered combinations of candidate inputs, i.e. (Q, LET, α_x/β_x), (Q, α_x/β_x) and (LET, α_x/β_x), were compared in terms of the difference between predicted and experimentally derived RBE_{2Gy}. The model taking (LET, α_x/β_x) showed significant ion dependence and worst performance and, thus, was abandoned. Compared to the model of (Q, α_x/β_x), predictions based on the model using (Q, LET, α_x/β_x) as input were not found to be better despite the additional information of LET. Considering that unnecessary input dimensions may degrade the data efficiency due to potential overfitting (Hastie *et al* 2009), the input of the final NN model proposed in this work was set to (Q, α_x/β_x). From a modeling point of view, the 'underlying assumption' of the models using (Q, α_x/β_x) and (LET, Q, α_x/β_x) can be regarded as 'RBE can be predicted given Q and α_x/β_x' and 'RBE can be predicted given LET, Q and α_x/β_x'. As particle type can be deduced if both Q and LET are given, the assumption of (LET, Q, α_x/β_x) model is equivalent to 'RBE can be predicted given particle type, LET and α_x/β_x', which is generally applied by most (ion-specific) LET-driven RBE models. The Q model was shown to have no worse performance compared to this kind of ion-specific LET model.

It is well-known that the application of NN models should be limited to interpolation. This limitation was clearly observed for the Q-driven NN RBE model. It can be seen in figure 5 that the model uncertainty in the Q-α_x/β_x domain covered by data points is much smaller (σ around 0.5) than the uncertainty in the remaining 'extrapolation' domain. Generally, model extrapolation should be treated cautiously, since the extrapolation of a model cannot be verified by experimental data. The same limitation applies to the model in terms of the dependence on dose and cell survival. Measures of the model prediction power, r2 and MSE, were shown to be better within a certain photon reference dose (2–4 Gy) or cell survival interval (near 10%). We believe this may be related to our inference that RBE values calculated in these domains are generally better supported by the consistency of experimental measurements (cf appendix). The currently resulting limitations do not prevent

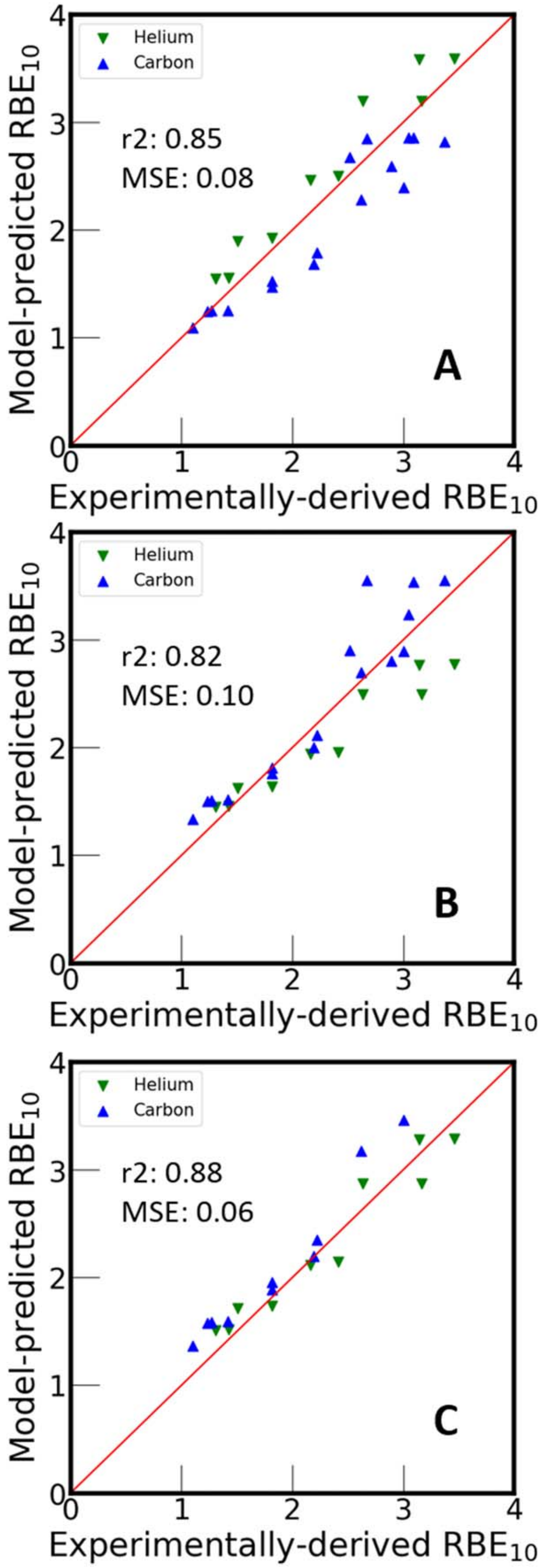

Figure 7. Comparison between experimentally derived RBE_{10} for helium and carbon irradiation of HSG cells and the predictions given by the LEM IV (a, full data), the Q-driven NN (b, full data) and the Q-driven linear model (c, only non-overkilling domain).

future improvement of the NN model in these domains, since data could eventually be measured in all domains of relevance and fed into the model. Moreover, this can also be seen as an advantage of the NN model since the prediction uncertainty can be used as an indicator of how strongly the model prediction was supported by the available experimental evidence.

The NN model provided RBE predictions that are comparable to those by LEM IV. The NN model relies primarily on experimental data rather than pre-knowledge of, e.g., microdosimetric dose distribution, detailed information on the cells, biological effect at extremely high dose (near the center of the ion track). This may allow the NN model to be more flexible and less demanding regarding the needed input data when trained in a clinical setting. In fact, the model was intentionally developed based on only two parameters, Q and $\alpha x/\beta x$, that are clinically accessible to enable clinical application in the future after successful clinical training and testing.

For the modeling of clinical RBE, factors beyond the physical and biological process within the cell should be considered including institute-specific factors, e.g. specific irradiation conditions and medical decisions (Karger and Peschke 2017). In this work, experimental details on, e.g., energy spectrum, secondary particles, institutional differences including biological protocols and the level of their specification vary between the records in the PIDE dataset. The data-driven Q model showed that the *in vitro* RBE is predictable in the domain of clinically relevant dose level by using only Q and α_x/β_x as input but without the need for a specific previously known formalism, e.g. the formulas used in most phenomenological models (Tilly *et al* 2005, Carabe-Fernandez *et al* 2007, Wedenberg *et al* 2013, McNamara *et al* 2015, Mairani *et al* 2017, McMahon 2021) and model parameters in mechanistic models (Hawkins 1998, Elsässer *et al* 2010). Going from an *in vitro* to a clinical endpoint, the use of Q and α_x/β_x as an input allows for flexible data-driven RBE modeling.

A systematic deviation between experimental data and the prediction for different ions was observed when the NN model was applied to predict the data reported by Furusawa *et al* (2000). This does not conflict with the conclusion of the ion-dependence test, as for this case, the NN model was trained on all data but those from one specific publication (Furusawa *et al* 2000), and then tested on this particular publication (Furusawa *et al* 2000). As training data and test data were divided systematically (one particular publication), a systematical error was not unexpected. This test design serves only as an example for the comparison with the other RBE models but is unsuited to test a systematic bias of the model. In addition, systematic deviations between the same experimental data and the predictions for LEM IV (Elsässer *et al* 2010) were observed, too.

Future work on Q modeling needs to focus on investigating how Q can be uniquely investigated in a spread-out Bragg peak as well as demonstrating the validity of the Q concept (i.e. the RBE of different particles follows the same trend when characterized by Q) for *in vivo* and clinical data. Yet, some clinical studies on brain toxicity associated with a variable RBE have emerged for patients treated with both protons (Bahn *et al* 2020, Eulitz *et al* 2019, 2023) and carbon ions (Koto *et al* 2014, Shirai *et al* 2017) and could be considered as a potential clinical endpoint of clinically related future studies.

Since Q is a relatively simple physical quantity, it can be easily implemented in treatment planning systems and used in place of LET in biological effectiveness guided treatment plan optimization that is emerging for proton therapy (Hahn *et al* 2022).

5. Conclusion

In this work, data-driven non-linear RBE modeling based on Q was proposed, analyzed and compared to experimental *in vitro* data as well as to a clinically applied RBE model. Using Q and α_x/β_x as input, the RBE at a clinically relevant dose range (2–4 Gy) can be predicted without explicit knowledge of ion type. This suggests the possibility of an empirical, ion-independent clinical RBE model that supports the transfer of RBE knowledge from better- to less well-studied ions, ultimately advancing clinical RBE research.

Data availability statement

No new data were created or analyzed in this study. Data will be available from 31 January 2023.

Appendix

The RBE, under a different definition, can be calculated using the linear-quadratic (LQ) model, which calculates the survival fraction (S) of cells at the dose level of D:

$$S = e^{-\alpha D - \beta D^2} \tag{A1}$$

where the α and β are model parameters.

Table A1. The performance of the models of $RBE_{dx}(Q, \alpha_x/\beta_x)$ at given photon reference dose, d_x, level of 0, 1, 2, 4 and 10 Gy. The RBE_{max}, i.e. α_i/α_x, is approximately regarded as RBE_{0Gy}. The performance is measured by the coefficient of determination (r2 score), mean square error (MSE) of the relative difference, p value of the ANOVA test.

d_x (Gy)	RBE_{dx} range	r2 score	MSE (relative error)	p (ANOVA)
0	0.72–27.84	0.85	0.86	0.27
1	0.86–9.69	0.79	0.39	0.47
2	0.95–6.24	0.77	0.30	0.58
4	0.98–4.26	0.75	0.22	0.18
10	0.91–2.96	0.65	0.19	0.72

The RBE_{dx} is the ratio of the dose of the reference photon d_x and the corresponding ion dose d_i that result in the same biological effectiveness which is described by formula (A1).

The RBE_{dx} can be calculated by:

$$RBE_{d_x} = d_x/d_i \tag{A2}$$

$$d_i = \frac{\sqrt{\beta_i^2 - 4\alpha_i \ln(s_x)} - \beta_i}{2\alpha_i} \tag{A3}$$

$$s_x = e^{-\alpha_x d_x - \beta_x d_x^2} \tag{A4}$$

where S_x is the survival fraction of corresponding photon irradiation, α_x, β_x, α_i and β_i are recorded in the PIDE.

The RBE_{10} is the ratio of the dose of reference photon dose d_x and the dose of the ion d_i when both result in 10% survival fraction. The RBE_{10} can be calculated by:

$$RBE_{10} = d_{x,10}/d_{i,10} \tag{A5}$$

$$d_{i,10} = \frac{\sqrt{\beta_i^2 - 4\alpha_i \ln(0.1)} - \beta_i}{2\alpha_i} \tag{A6}$$

$$d_{x,10} = \frac{\sqrt{\beta_x^2 - 4\alpha_x \ln(0.1)} - \beta_x}{2\alpha_x} \tag{A7}$$

While the experimentally derived RBE_{10} was calculated using the α_x, β_x, α_i and β_i recorded in the PIDE, the RBE_{10} predicted by the linear model was calculated using the α_x and β_x recorded in the PIDE and the α_i and β_i predicted by the model:

$$\alpha_i = RBE_{max}\,\alpha_x \tag{A8}$$

$$\beta_i = RBE_{min}^2\,\beta_x \tag{A9}$$

$$RBE_{max} = 1 + k_Q \cdot \frac{Q}{\alpha_x/\beta_x} \tag{A10}$$

$$RBE_{min} = 1 \tag{A11}$$

where $k_Q = 15.5$ A·MeV·Gy (Tian *et al* 2022).

The performance of the NN model predicting RBE_{dx} at d_x levels of 0, 1, 2, 4 and 10 Gy as well as RBE_S at cell survival *S* of 0.1%, 1.0%, 10.0%, 50.0% and 90.0% was compared using the same training (80%) and test (20%) data sets.

As the magnitudes of the experimentally derived RBE at different d_x or survival level are different (cf tables A1 and A2, respectively), the MSE of the relative error, instead of the error values discussed in the manuscript, were used for comparison. Other evaluation metrics, i.e. r2 score and ANOVA tests are compared as well. The results are shown in tables A1 and A2. Considering the r2 score and MSE (relative) tradeoff, the performance of the model was considered to be better for d_x between 2-4 Gy and cell survival around 10%, this is consistent to the result of correlation analysis (cf figure 2).

Note that the experimentally derived RBE is calculated using PIDE-recorded α and β values, which were obtained by fitting the measured cell survival data points using the LQ model. However, the obtained values for α and β also depend on the applied fitting conditions. Refitting the same experimentally measured data points, the PIDE group obtained and recorded also different sets of α and β values. The resulting effect on experimentally derived RBE values was measured by comparing the two RBE values calculated either based on an α & β set fitted by the original experimenters or by the PIDE group. For a quantitative comparison, the r2 score between the two experimentally derived RBE values was applied at different levels of dose and cell survival. The result is shown in figure A1. Note that no RBE modeling is involved in this analysis.

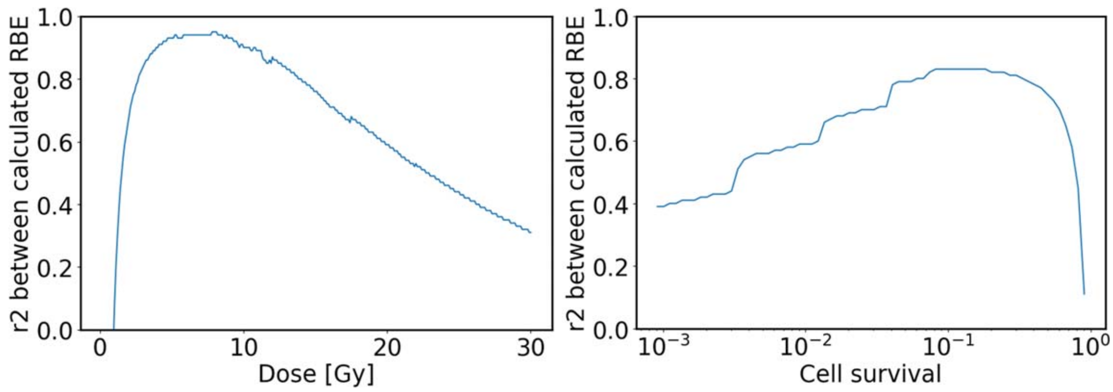

(a) (b)

Figure A1. The coefficient of determination (r2) of the RBE calculated using the PIDE and original alpha–beta sets for the same experiments. The RBE shown on the left and right are defined by the endpoints reference photon dose d_x and given cell survival, respectively.

Table A2. The performance of the models of $RBE_S(Q, \alpha_x/\beta_x)$ at cell survival fractions S of 0.1%, 1.0%, 10.0%, 50.0% and 90.0%. The performance is measured by: coefficient of determination (r2 score), mean square error (MSE) of the relative difference, p value of ANOVA test.

Survival fraction (%)	RBE_{dx} range	r2 score	MSE (relative error)	p (ANOVA)
0.1	0.42–3.48	0.57	0.17	0.61
1.0	0.49–3.62	0.77	0.16	0.68
10.0	0.63–4.53	0.83	0.19	0.86
50.0	0.86–6.12	0.79	0.24	0.85
90.0	0.66–9.66	0.74	0.44	0.63

The r2 score was observed to be highest in the domain of 2–4 Gy or cell survival around 10%, which is consistent with the domain that our model showed better prediction.

We believe that the cell survival curves reproduced by different sets of fitted α & β values should converge (high r2 score) where there are sufficient experimental measurements, while diverging (low r2 score) where measurements may be insufficient. Thus, it can be inferred that, generally, the RBE values calculated in the domains of higher r2 scores are more likely to be confirmed by direct experimental evidence as cell survival curves obtained by different groups are consistent in those domains.

ORCID iDs

Liheng Tian https://orcid.org/0000-0003-1795-7768
Armin Lühr https://orcid.org/0000-0002-9450-6859

References

Ando K and Kase Y 2009 Biological characteristics of carbon-ion therapy *Int. J. Radiat. Biol.* **85** 715–28

Baggio L, Cavinato M, Cherubini R, Conzato M, Cucinotta F, Favaretto S, Gerardi S, Lora S, Stoppa P and Williams J R 2002 Relative biological effectiveness of light ions in human tumoural cell lines: role of protein p53 *Radiat. Prot. Dosimetry* **99** 211–4

Bahn E, Bauer J, Harrabi S, Herfarth K, Debus J and Alber M 2020 Late contrast enhancing brain lesions in proton-treated patients with low-grade glioma: clinical evidence for increased periventricular sensitivity and variable RBE *Int. J. Radiat. Oncol. Biol. Phys.* **107** 571–8

Carabe-Fernandez A, Dale R G and Jones B 2007 The incorporation of the concept of minimum RBE (RBE min) into the linear-quadratic model and the potential for improved radiobiological analysis of high-LET treatments *Int. J. Radiat. Biol.* **83** 27–39

Chang D S, Lasley F D, Das I J, Mendonca M S and Dynlacht J R 2014 Oxygen effect, relative biological effectiveness and linear energy transfer *Basic Radiotherapy Physics and Biology*. (Cham: Springer) pp 235–40

Connor M *et al* 2017 Regional susceptibility to dose-dependent white matter damage after brain radiotherapy *Radiother. Oncol.* **123** 209–17

Dale R G, Jones B and Cárabe-Fernández A 2009 Why more needs to be known about RBE effects in modern radiotherapy *Appl. Radiat. Isot.* **67** 387–92

Ebner D K, Frank S J, Inaniwa T, Yamada S and Shirai T 2021 The emerging potential of multi-ion radiotherapy *Front. Oncol.* **11** 624786

Elsässer T *et al* 2010 Quantification of the relative biological effectiveness for ion beam radiotherapy: direct experimental comparison of proton and carbon ion beams and a novel approach for treatment planning *Int. J. Radiat. Oncol.* **78** 1177–83

Eulitz J *et al* 2023 Increased relative biological effectiveness and periventricular radiosensitivity in proton therapy of glioma patients *Radiother. Oncol.* **178** 109422

Eulitz J *et al* 2019 Predicting late magnetic resonance image changes in glioma patients after proton therapy *Acta Oncol.* **58** 1536–9

Friedrich T, Pfuhl T and Scholz M 2021 Update of the particle irradiation data ensemble (PIDE) for cell survival *J. Radiat. Res. (Tokyo)* **62** 645–55

Friedrich T, Scholz U, Elsässer T, Durante M and Scholz M 2012 Calculation of the biological effects of ion beams based on the microscopic spatial damage distribution pattern *Int. J. Radiat. Biol.* **88** 103–7

Furusawa Y, Fukutsu K, Aoki M, Itsukaichi H, Eguchi-Kasai K, Ohara H, Yatagai F, Kanai T and Ando K 2000 Inactivation of aerobic and hypoxic cells from three different cell lines by accelerated ^{3}He-, ^{12}C- and ^{20}Ne-ion beams *Radiat. Res.* **154** 485–96

Geissel H, Weick H, Scheidenberger C, Bimbot R and Gardès D 2002 Experimental studies of heavy-ion slowing down in matter *Nucl. Instrum. Methods Phys. Res. Sect. B Beam Interact. Mater. At.* **195** 3–54

Hahn C, Heuchel L, Ödén J, Traneus E, Wulff J, Plaude S, Timmermann B, Bäumer C and Lühr A 2022 Comparing biological effectiveness guided plan optimization strategies for cranial proton therapy: potential and challenges *Radiat. Oncol.* **17** 169

Hastie T, Tibshirani R and Friedman J 2009 *The Elements of Statistical Learning: Data Mining, Inference, and Prediction.* (New York, NY: Springer Science & Business Media)

Hawkins R 1998 A microdosimetric-kinetic theory of the dependence of the RBE for cell death on LET *Med. Phys.* **25** 1157–70

Hawkins R B 1996 A microdosimetric-kinetic model of cell death from exposure to ionizing radiation of any LET, with experimental and clinical applications *Int. J. Radiat. Biol.* **69** 739–55

Heuchel L, Hahn C, Pawelke J, Sørensen B S, Dosanjh M and Lühr A 2022 Clinical use and future requirements of relative biological effectiveness: Survey among all European proton therapy centres *Radiotherapy and Oncology* **172** 134–9

Karger C P and Peschke P 2017 RBE and related modeling in carbon-ion therapy *Phys. Med. Biol.* **63** 01TR02

Kase Y, Kanai T, Matsufuji N, Furusawa Y, Elsässer T and Scholz M 2008 Biophysical calculation of cell survival probabilities using amorphous track structure models for heavy-ion irradiation *Phys. Med. Biol.* **53** 37–59

Koto M, Hasegawa A, Takagi R, Fujikawa A, Morikawa T, Kishimoto R, Jingu K, Tsujii H and Kamada T 2014 Risk factors for brain injury after carbon ion radiotherapy for skull base tumors *Radiother. Oncol. J. Eur. Soc. Ther. Radiol. Oncol.* **111** 25–9

Lambrecht M, Eekers D B P, Alapetite C, Burnet N G, Calugaru V, Coremans I E M, Fossati P, Høyer M and A J 2018 Radiation dose constraints for organs at risk in neuro-oncology; the European Particle Therapy Network consensus *Radiother. Oncol.* **128** 26–36

Lühr A, Toftegaard J, Kantemiris I, Hansen D C and Bassler N 2012 Stopping power for particle therapy: The generic library libdEdx and clinically relevant stopping-power ratios for light ions *Int. J. Radiat. Biol.* **88** 209–12

Lühr A, von Neubeck C, Helmbrecht S, Baumann M, Enghardt W and Krause M 2017 Modeling *in vivo* relative biological effectiveness in particle therapy for clinically relevant endpoints *Acta Oncol.* **56** 1392–8

Mairani A, Dokic I, Magro G, Tessonnier T, Bauer J, Böhlen T, Ciocca M, Ferrari A, Sala P, Jäkel O *et al* 2017 A phenomenological relative biological effectiveness approach for proton therapy based on an improved description of the mixed radiation field *Phys. Med. Biol.* **62** 1378

McMahon S J 2021 Proton RBE models: commonalities and differences *Phys. Med. Biol.* **66** 04NT02

McNamara A L, Schuemann J and Paganetti H 2015 A phenomenological relative biological effectiveness (RBE) model for proton therapy based on all published *in vitro* cell survival data *Phys. Med. Biol.* **60** 8399

Mein S *et al* 2019 Biophysical modeling and experimental validation of relative biological effectiveness (RBE) for 4He ion beam therapy *Radiat. Oncol.* **14** 123

Mizoe J *et al* 2012 Results of carbon ion radiotherapy for head and neck cancer *Radiother. Oncol.* **103** 32–7

Paganetti H *et al* 2019 Report of the AAPM TG-256 on the relative biological effectiveness of proton beams in radiation therapy *Med. Phys.* **46** e53–e78

Pedregosa F *et al* 2011 Scikit-learn: Machine Learning *in Python. J. Mach. Learn. Res.* **12** 2825–30

Raju M R and Carpenter S G 1978 A heavy particle comparative study. Part IV: acute and late reactions *Br. J. Radiol.* **51** 720–7

Reback J *et al* 2022 pandas-dev/pandas: Pandas 1.4.0rc0.

Scholz M, Kellerer A, Kraft-Weyrather W and Kraft G 1997 Computation of cell survival in heavy ion beams for therapy *Radiat. Environ. Biophys.* **36** 59–66

Shirai K *et al* 2017 Dose–volume histogram analysis of brainstem necrosis in head and neck tumors treated using carbon-ion radiotherapy *Radiother. Oncol.* **125** 36–40

Tian L, Hahn C and Lühr A 2022 An ion-independent phenomenological relative biological effectiveness (RBE) model for proton therapy *Radiother. Oncol.* **174** 69–76

Tilly N, Johansson J, Isacsson U, Medin J, Blomquist E, Grusell E and Glimelius B 2005 The influence of RBE variations in a clinical proton treatment plan for a hypopharynx cancer *Phys. Med. Biol.* **50** 2765

Underwood T S A, McNamara A L, Appelt A, Haviland J S, Sørensen B S and Troost E G C 2022 A systematic review of clinical studies on variable proton Relative Biological Effectiveness (RBE *Radiother. Oncol.* **175** 79–92

Wedenberg M, Lind B K and Hardemark B 2013 A model for the relative biological effectiveness of protons: the tissue specific parameter α/β of photons is a predictor for the sensitivity to LET changes *Acta Oncol.* **52** 580–8